Since January 2020 Elsevier has created a COVID-19 resource centre with free information in English and Mandarin on the novel coronavirus COVID-19. The COVID-19 resource centre is hosted on Elsevier Connect, the company's public news and information website.

Veterinary Microbiology 175 (2015) 157–166

Contents lists available at ScienceDirect

Veterinary Microbiology

journal homepage: www.elsevier.com/locate/vetmic

Levels of feline infectious peritonitis virus in blood, effusions, and various tissues and the role of lymphopenia in disease outcome following experimental infection

Niels C. Pedersen [a,*], Chrissy Eckstrand [c], Hongwei Liu [a], Christian Leutenegger [b], Brian Murphy [c]

[a] Center for Companion Animal Health, School of Veterinary Medicine, University of California, Davis, CA, USA
[b] IDEXX Laboratories, Sacramento, CA, USA
[c] Department Pathology, Microbiology and Immunology, School of Veterinary Medicine, University of California, Davis, CA, USA

ARTICLE INFO

Article history:
Received 11 August 2014
Received in revised form 16 October 2014
Accepted 27 October 2014

Keywords:
FIP virus
Experimental
RT-qPCR
Immunohistochemistry
Macrophages
Viremia

ABSTRACT

Twenty specific pathogen free cats were experimentally infected with a virulent cat-passaged type I field strain of FIPV. Eighteen cats succumbed within 2–4 weeks to effusive abdominal FIP, one survived for 6 weeks, and one seroconverted without outward signs of disease. A profound drop in the absolute count of blood lymphocytes occurred around 2 weeks post-infection (p.i.) in cats with rapid disease, while the decrease was delayed in the one cat that survived for 6 weeks. The absolute lymphocyte count of the surviving cat remained within normal range. Serum antibodies as measured by indirect immunofluorescence appeared after 2 weeks p.i. and correlated with the onset of disease signs. Viral genomic RNA was either not detectable by reverse transcription quantitative real-time PCR (RT-qPCR) or detectable only at very low levels in terminal tissues not involved directly in the infection, including hepatic and renal parenchyma, cardiac muscle, lung or popliteal lymph node. High tissue virus loads were measured in severely affected tissues such as the omentum, mesenteric lymph nodes and spleen. High levels of viral genomic RNA were also detected in whole ascitic fluid, with the cellular fraction containing 10–1000 times more viral RNA than the supernatant. Replicating virus was strongly associated with macrophages by immunohistochemistry. Virus was usually detected at relatively low levels in feces and there was no evidence of enterocyte infection. Viral genomic RNA was not detected at the level of test sensitivity in whole blood, plasma, or the white cell fraction in terminal samples from the 19 cats that succumbed or in the single survivor. These studies reconfirmed the effect of lymphopenia on disease outcome. FIPV genomic RNA was also found to be highly macrophage associated within diseased tissues and effusions as determined by RT-qPCR and immunohistochemistry but was not present in blood.

1. Introduction

In spite of many decades of studies on experimental FIPV infection, there is very little information on how the virus and host interact over an entire disease course. Many experimental FIPV infection studies have also been limited to the final disease outcome, e.g., the testing of vaccine candidates for efficacy or testing of various types and biotypes of feline coronavirus isolates for disease potential (Pedersen, 2009, 2014a). Still other experimental studies have concentrated on specific virus- or host-related inflammatory or immune responses, also measured mainly

* Corresponding author at: University of California, One Shields Avenue, Davis, CA 95616, USA; Tel.: +1 530 752 7402; fax: +1 530 752 7701.
E-mail address: ncpedersen@ucdavis.edu (N.C. Pedersen).

http://dx.doi.org/10.1016/j.vetmic.2014.10.025
0378-1135/

in terminally ill cats (Pedersen, 2014a). There are several longitudinal studies which have followed the entire disease course, but these studies were concerned mainly with disease signs such as fever, antibody responses and cytokine expression and not with viral loads in various tissues (Pedersen and Boyle, 1980; Weiss and Scott, 1981; Gunn-Moore et al., 1998a). Only one other temporal study has been performed on FIPV levels in peripheral blood of experimentally infected cats (de Groot-Mijnes et al., 2005). Although the authors suggested that there was a significant viremia associated with disease, viremia was erratic, observed mainly at week one post-infection and terminally, and the levels of viral genomic RNA, even when detected, were never high.

There has been a long standing belief that FIPV is not shed from the body, at least to the very high levels seen in FECV infection or in an infectious form (Pedersen et al., 2009). FIPV does not appear to replicate in enterocytes (Chang et al., 2010; Pedersen et al., 2012), and was first associated with macrophages by electron microscopy and immunohistochemistry (Ward, 1970; Pedersen and Boyle, 1980). Dean et al. (2003) studied the distribution of FIPV by immunofluorescence at the time of death in experimentally infected cats and also found macrophages to be heavily infected in mediastinal and mesenteric lymph nodes and spleen, with much less evidence of infection in peripheral tissues such as popliteal and cervical lymph nodes and bone marrow.

Lymphopenia is a consistent feature of both naturally (Pedersen, 2009, 2014b) and experimentally induced-FIP (Dean et al., 2003; de Groot-Mijnes et al., 2005). The role of lymphopenia in FIP has not been determined, but it has been equated with a decrease in cellular immunity and ultimate disease outcome in experimental infections (de Groot-Mijnes et al., 2005; Vermeulen et al., 2013). Although lymphopenia appears to play a role in FIP, temporal studies on the appearance, magnitude and duration of lymphopenia in cats that succumb or survive experimental infection have not been reported; most cell counts have been taken prior to infection and terminally.

The emphasis of FIP diagnostics has long been on developing a simple blood test that would reliably and specifically detect the causative virus (Pedersen, 2014b). Herrewegh et al. (1995) reported on the detection of viral RNA in blood serum or plasma of cats experimentally and naturally infected with FIPV using a nested RT-PCR that amplified a sequence within the 3′-UTR that was highly conserved among 10 different FIPV and FECV isolates. They were able to detect feline coronavirus RNA in the serum, plasma or ascitic fluid of 14/18 cats with naturally occurring FIP. Unfortunately, they were also able to detect viral RNA in the plasma of 2/7 healthy cats that were concurrently shedding FECV in their feces. An attempt was made to eliminate this problem of specificity by developing an RT-PCR that would only measure forms of coronavirus mRNA that were replication competent (Simons et al., 2005). The rationale was that FECV would not replicate in the blood; therefore, the replicative form of genomic RNA would only be found in the blood of cats with FIP. The authors reported that this test was highly accurate in identifying cats with FIP. Shortly thereafter additional studies using the same assay demonstrated replicating forms of RNA in the blood of healthy cats infected with FECV (Can-Sahna et al., 2007; Kipar et al., 2010), casting doubts on the specificity of such tests. The ability of FECV to replicate in blood monocyte/macrophages was also reported by other groups (Vogel et al., 2010). Chang et al. (2012) subsequently identified two specific mutations within the fusion peptide of the spike protein of FIPVs that were not present in parent FECVs. These would seem to be logical mutations to incorporate into a RT-qPCR. However, a more recent study by Porter et al. (2014) demonstrated the presence of coronavirus with the FIPV-specific fusion peptide mutation in tissues of healthy cats. They concluded that the spike fusion region specific mutation was an adaptation of FECV for growth in blood monocyte/macrophages and not directly related to disease. However, all of these various tests and objections are moot if FIPV genomic RNA is not consistently present in detectable levels by RT-qPCR in blood or blood fractions in cats with FIP.

The goal of this study was to temporally correlate disease signs in experimental FIPV infection with lymphopenia, antibody response, and viremia with disease outcome (death or survival) and specific cell and organ localization of virus in terminal tissue samples by RT-qPCR and immunohistochemistry. We will show that lymphopenia is the strongest predictor of disease outcome, virus is strongly associated with macrophages in lesional tissues and effusions, and viremia is not detectable at any stage of the infection even using a highly sensitive RT-qPCR.

2. Materials and methods

2.1. Experimental animals

Specific pathogen free cats were bred in the facilities of the Feline Research Laboratory (FRL), Center for Companion Animal Health, UC Davis under IACUC #16989. Cats used in this study were part of a larger experiment concerned with natural immunity (Pedersen et al., 2014) and were 6–9 months of age and equally intact male and female. They were housed in the FRL and cared for by FRL staff under ultimate authority of the Campus Veterinary Services.

2.2. Experimental FIPV infection

Cats were infected with a cat-passaged type I field isolate of FIPV (FIPV-m3c-2) (Pedersen et al., 2009), which has a functional mutation in the 3c gene and would not be expected to actively replicate in the intestinal epithelium (Chang et al., 2010; Pedersen et al., 2012). The inoculum was prepared as a cell-free suspension of diseased omentum (starting at 25 g/100 ml) that underwent differential centrifugation to remove particulate matter, bacteria and subcellular debris and then stored at −60 °C. It was diluted 1:80 in Hanks buffered saline prior to use and two ml was injected intraperitoneally to infect each cat. The final inoculate contained 4.32×10^5 viral genomes as determined by RT-qPCR. Cats were infected under IACUC

protocol #16637 and monitored for disease signs and euthanatized when their disease status was deemed clinically terminal, usually within 2–4 weeks of infection.

2.3. Sample collection

Blood samples were taken at weekly intervals and a gross necropsy performed at the time of death. Blood and tissue samples were harvested and archived for this and future studies.

2.4. Blood cell counts

Whole blood was diluted 1:10 with RBC lysis solution (Qiagen, Valencia, CA), and total white blood counts were done microscopically with a hematocytometer. Slides of blood smears were stained using a Differential Quick Stain Kit (Modified Giemsa) (Polysciences, Inc., Warrington, PA) and differential cell counts performed manually.

2.5. Histopathology and immunohistochemistry

Samples of tissues obtained at necropsy were immediately placed in 10% buffered formalin and fixed for 24 h before being routinely embedded into paraffin blocks. Tissues that were examined histologically (all cats) and by immunohistochemistry (two cats) included liver, spleen, kidney, mesenteric lymph node, omentum, ileum, caecum, heart, and lungs.

Immunohistochemistry was performed on 4 μm serial sections of formalin fixed and paraffin embedded tissues using a streptavidin biotin detection system (Biocare Medical, Concord, CA). Mouse monoclonal antibodies to FIPV (Custom Monoclonal International, clone FIPV3-70, 1:200), CD18 (Peter Moore, UC Davis, clone Fe3.9F2), and CD3 (Peter Moore, UC Davis, clone CD3-12) were used with some modifications. Before applying the primary antibodies, slides were steam pretreated in citrate buffer (Dako S1699) at 98 °C for 20 min followed by a 20 min cooling. They were then washed in PBS and blocked with 10% normal horse serum for 20 min. Amino ethyl carbazole (AEC, Dako Corp.) was used as the chromogen sections were counterstained with Mayer's hematoxylin. Substituting a matched mouse IgG correlate for the primary antibody served as the negative control.

2.6. Ascites macrophage isolation and immunocytochemistry

Viable ascites macrophages were isolated by positive immunomagnetic selection columns (MACS MicroBeads, Miltenyi Biotec) and anti-CD11b (Peter Moore, UC Davis, clone CA16.3E10-IgG1) following manufacturers protocols. Enriched cells were deposited on a glass slide using cytocentrifugation (Cytospin 4; Thermo Shandon). Immunocytochemistry for Coronavirus was performed as described above with the following modifications: primary antibody dilution 1:100 and no antigen retrieval step. Virally infected Fcwf-4 cells (ATCC) and uninfected cells were used as positive and negative controls.

2.7. RT-qPCR for virus quantitation

FIPV genomic RNA was detected using a RT-qPCR directed to a region of the accessory 7b gene according to a published procedure (Gut et al., 1999). RNA integrity and quantity was assessed in parallel with an 18S rRNA based Real-time PCR test. The specificity of the fluorogenic RT-PCR was confirmed by sequencing the plasmid pT7-StFCoV by the chain termination method (Microsynth, Balgach, Switzerland). The Real-time PCR was run with three contamination controls including regular negative controls, negative extraction controls and laboratory monitoring for the absence of random positive PCR signals. To eliminate PCR product carry over, all reactions included the AmpErase UNG system (Pang et al., 1992). Absence of PCR inhibition is confirmed by using a spike-in internal positive control. This procedure was reportedly 10–100 times more sensitive in detecting FIPV mRNA than that achieved with a nested RT-PCR that was described earlier (Herrewegh et al., 1995). The sensitivity of the assay plotting cycle threshold (CT) values against FIPV genomic RNA copy numbers is shown in Fig. 1. At 40 cycles, considered the upper limit of meaningful amplification for RT-qPCR, the assay was capable of detecting ~1000 mRNA copies/ml of fluid or g of tissue.

3. Results

3.1. Clinical responses

The first clinical sign of disease was observed at around 2 weeks post-infection and consisted of a fever ranging from 30.3 °C to 40.9 °C in 18 of the 20 cats (Fig. 2). A more undulating fever was observed in one other cat (#31) starting at around 2 weeks post-infection but it did not become persistent until week 6. A final cat (#26) was febrile (39.5 °C) only on day 19. The onset of fever was followed by increasing inappetance, jaundice, bilirubinuria, hyperbilirubinemia, and abdominal effusion in 19 of the 20 cats. The one surviving cat demonstrated no clinical signs of disease. In accordance with the IACUC protocol,

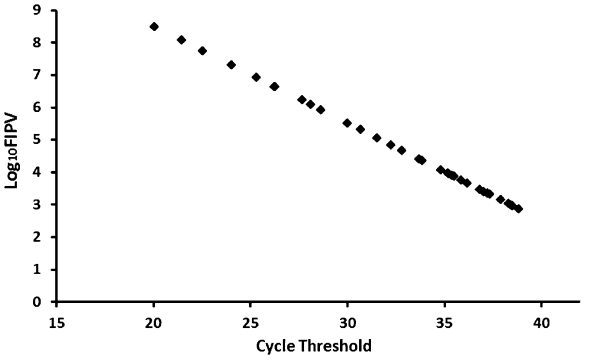

Fig. 1. Sensitivity of the RT-qPCR used in this study to detect FIPV genomes.

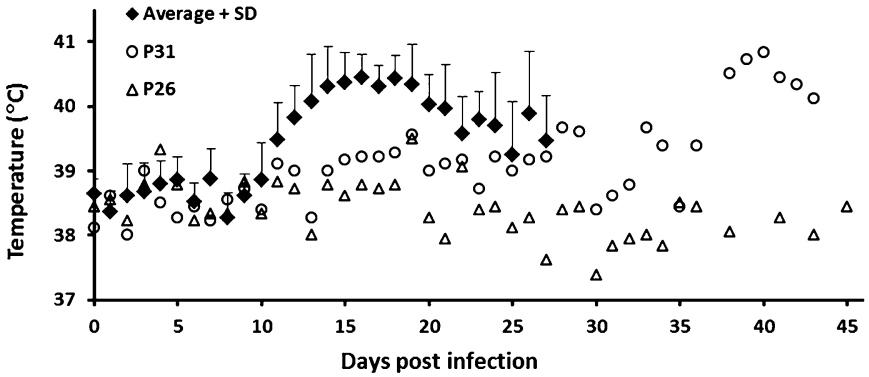

Fig. 2. Febrile responses of cats that were experimentally infected with FIPV.

18 cats were euthanatized at post-infection days 14–28, one cat (#31) survived until week 6, and one cat (#26) showed no clinical signs of disease through week 6 and has remained healthy up to the time of this submission (>7 months) (Table 1).

Diarrhea of a moderate to severe nature was noticed pre-mortem in the litterboxes of some of the cats, usually beginning 2–3 weeks post-infection. Diarrheic, non-odorous, bile-tinged stool with excess gas and mucus was identified in both the small and large intestine in 11/19 cats at necropsy. Feces from the remaining cats were of normal form and consistency.

3.2. Serum antibody responses

Feline coronavirus-specific antibodies, as measured by IFA, appeared in the serum between 2 and 3 weeks post-infection and rose to terminal titers of 1:100–1:400 or higher (Fig. 3). The appearance of antibodies in the serum correlated with the onset of disease signs (Figs. 2 and 3).

3.3. Hematology

The total white blood cell count decreased somewhat over the 2–6 week observation period in the 19 cats that

Table 1
RT-qPCR CT values for FIPV genomic RNA in whole blood, plasma, and WBC fraction of experimentally infected cats during the six week post-infection period.

Days	Cat																			
	P25	P26	P27	P28	P29	P30	P31	P32	P33	P34	P35	P36	P37	P38	P39	P40	P41	P42	P43	P44
	D15[a]		D15[a]	D14[a]	D20[a]	D20[a]	D42[a]	D26[a]	D14[a]	D26[a]	D15[a]	D26[a]	D23[a]	D20[a]	D26[a]	D20[a]	D22[a]	D18[a]	D19[a]	D14[a]
Plasma																				
0	–	–	37	–	–	–	–	–	–	–	–	–	–	–	–	–	–	39	–	–
7	–	–	–	–	–	–	–	–	–	–	–	–	–	–	–	–	–	–	–	–
14	–	–	–	–[b]	–	–	–	–	–[b]	–	–	–	–	–	–	–	–	–	–	40[b]
	–[b]		–[b]		–[b]	40[b]					–[b]			–[b]		–[b]		–[b]	–[b]	
21		–					–	–		–		–	–		–					
													–[b]				–[b]			
26		–					–	–[b]		–[b]		–[b]			40[b]					
42		–					–[b]													
Whole blood																				
0	–	–	–	–	–	–	–	–	–	–	–	–	–	–	–	–	–	–	–	–
7	–	–	–	–	–	–	38	–	–	–	–	–	–	–	–	–	–	–	–	37[b]
14	–	–	–	–[b]	–	–	–	–	–[b]	–	–	–	–	–	–	–	–	39	–	38[b]
	–[b]		38[b]		–[b]	–[b]					39[b]					40[b]		40[b]	–[b]	
21		–					–	–		–		–	–	–[b]	–		–[b]			
													–[b]							
26		–					–	–[b]		37[b]		–[b]			–[b]					
42		–					–[b]													
WBC																				
0	–	–	–	–	–	–	–	–	–	–	–	–	–	–	–	37	–	–	–	–
7	–	–	–	–	–	–	–	–	–	–	–	–	–	–	–	–	–	38	–	36
14	–	–	–	–[b]	–	–	–	–	40[b]	–	–	–	–	40	–	–	–	–	–	–[b]
	–[b]		38[b]		–[b]	–[b]					–[b]			–[b]		40[b]		38[b]	–[b]	
21		–					–	–		–		–	–		–		–[b]			
													37[b]							
26		–					–	–[b]		37[b]		38[b]			38[b]					
42		–					40[b]													

[a] Euthanized.
[b] Terminal CT value.

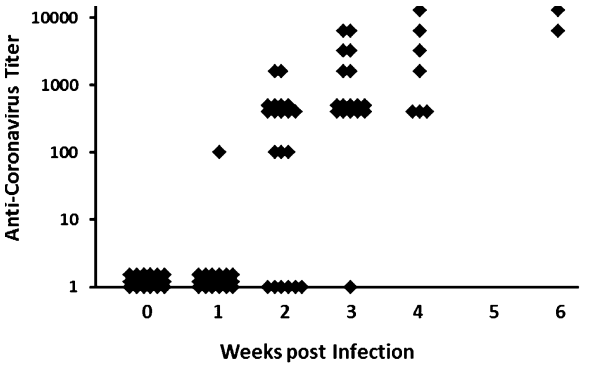

Fig. 3. Anti-feline coronavirus titers in plasma of cats experimentally infected with FIPV.

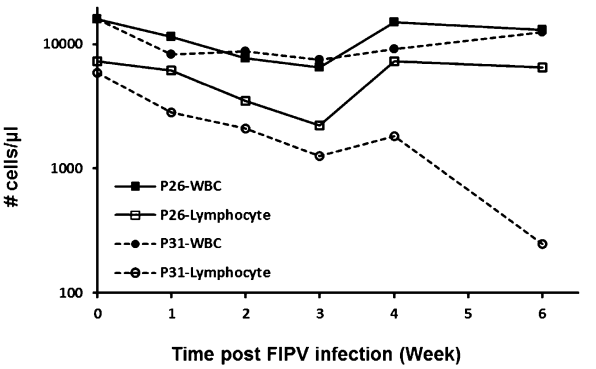

Fig. 5. Absolute total white blood cell and lymphocyte counts of two cats experimentally infected with FIP, one (p26) of which resisted disease and one (p31) that died at 6 weeks post-infection.

developed FIP (Fig. 4). A profound lymphopenia occurred starting at around 2–4 weeks post-infection and correlated with the disease course (Fig. 4). The earlier lymphopenia occurred post-infection, the more rapid the disease course. The one cat (P31) that survived 6 weeks did not become severely lymphopenic until after week 4, while the one surviving cat (P26) never became lymphopenic (Fig. 5). Gross bilirubinuria and jaundice correlated with disease course, appearing earlier in cats with more rapid disease.

3.4. Gross pathology

A diffuse peritonitis with effusion of 30–300 ml of viscid, yellow-tinged, cloudy fluid was present at necropsy. The omentum and gastro-splenic mesentery manifested severe vascular congestion, edema, and serous atrophy of fat (Fig. 6). Intestinal mesenteries, abdominal serosa, and capsular surfaces of abdominal organs were less severely affected. Surface orientated plaques, <1 to several mm in size, were a characteristic feature of the inflammation (Fig. 6). Fibrin tags were free in the abdomen and common on the spleen and liver margins. The spleen, caecum and caecal-colic/mesenteric lymph nodes were frequently enlarged. The liver appeared grossly normal below the capsule in all but two affected cats, which demonstrated 0.5–1 mm whitish foci throughout the parenchyma. The kidneys were not grossly involved below the level of the capsule. The lungs, heart and other thoracic tissues appeared normal in 15/19 cats necropsied. The remaining four cats had signs of mediastinitis with enlargement of the sternal lymph nodes. The pericardium was thickened with an increased amount of pericardial fluid in two of these cats. The popliteal lymph nodes were normal in size and appearance.

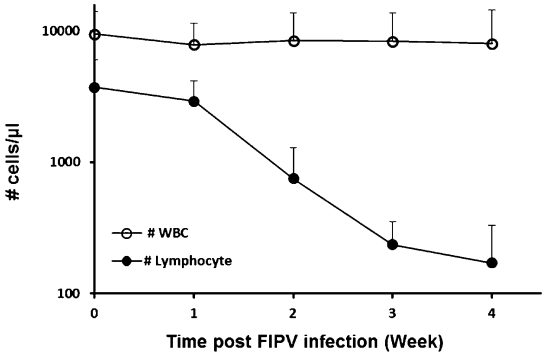

Fig. 4. Absolute total white cell and lymphocyte counts of 18 cats that died within 2–4 weeks following experimental infection with FIPV.

3.5. Histopathology and immunohistochemistry

Histologic lesions were common to all of the cats and included pyogranulomatous vasculitis of the omentum (Fig. 7), mesentery, visceral peritoneal surface of the spleen, liver, mesenteric lymph node, caecum, and ileum; predominantly histocytic, neutrophilic, and fibrinous peritonitis; serous atrophy of omental fat (Fig. 7); subcapsular splenic histiocytosis; splenic neutrophilia and ellipsoid hyperplasia. Abnormalities not uniformly observed in all cats included pyogranulomatous lymphadentitis and necrosis in the mesenteric lymph nodes and caecal and ileal Peyers

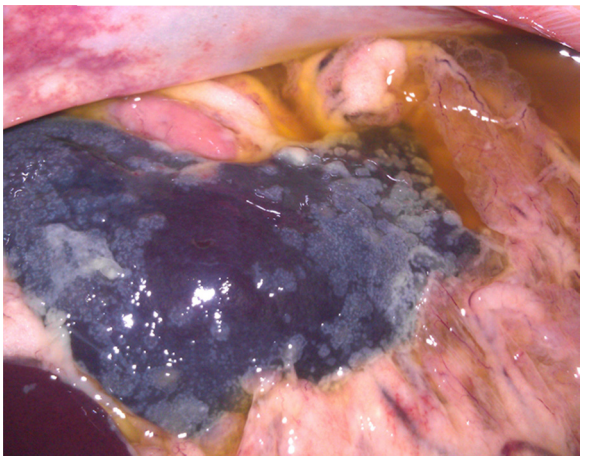

Fig. 6. Gross appearance of the abdomen in a cat with experimentally induced effusive FIP. The omentum is edematous, omental vessels prominent and reddened, the surface of the spleen is covered with whitish plaques (pyogranulomas) and fibrin, and the abdomen is filled with a yellowish exudate.

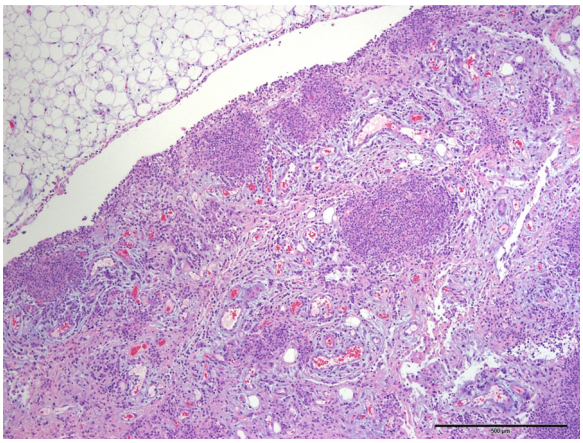

Fig. 7. Omentum (Hematoxylin and Eosin). The omentum is greatly expanded by pyogranulomatous inflammatory nodules and peritoneal inflammation. Blood vessels are prominent and there is multifocal serous atrophy of fat.

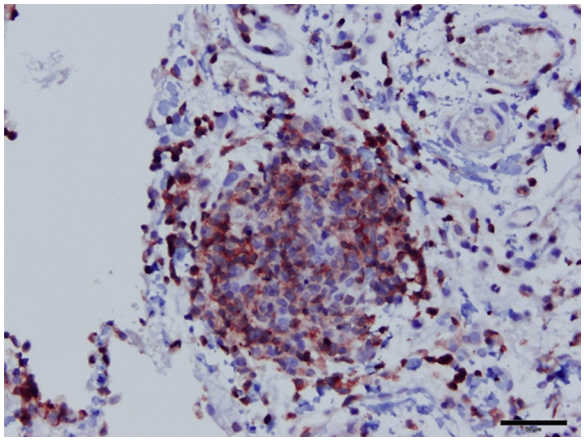

Fig. 9. Omentum (Immunoperoxidase). High magnification of an omental pyogranuloma demonstrates a predominance of strongly CD18 positive macrophages (400×).

patches; pyogranulomatous vasculitis of the caecal and ileal wall with associated local peritonitis; lymphoid hyperplasia of mesenteric lymph nodes; and pyogranulomatous hepatitis. The lungs and heart, with the exception of the pericardium and mediastinum in several cats, appeared to be unaffected by gross examination. No gross or clinical signs of ocular or neurologic disease were observed and tissues from these organs were therefore not studied.

Immunohistochemistry for feline coronavirus antigen, CD18, and CD3 were performed on these same tissues from two of the 19 cats. Immunoperoxidase staining demonstrated the presence of cell-associated feline coronavirus antigen within pyogranulomas and on the peritoneal surface (Fig. 8). Pyogranulomas contained a predominance of cells staining strongly positive for CD18, a characteristic of macrophages (Fig. 9), and lower proportions of CD3 positive T-lymphocytes and typical neutrophils (Fig. 10). Viral antigen was found exclusively in the large foamy macrophage-like cells (Fig. 11). Enterocytes of the caecum and ileum were uniformly negative for feline coronavirus antigen, while cells in the inflammatory reaction on the serosal surface stained positive (Fig. 12).

3.6. Immunomagnetic isolation CD11b cells from ascites and immunocytochemistry

In order to confirm that FIPV was replicating exclusively in macrophages, cells positive for the CD11b cell surface marker were isolated from the ascites fluid of one of the cats. Both neutrophils and macrophages were isolated in pure form as expected, given that CD11b is present on the surface membranes of both cell types. Positive staining for FIPV antigen was limited to the large mononuclear cell population, while neutrophils did not stain (Fig. 13).

3.7. FIPV genomic RNA levels in tissues, feces, ascites and blood

FIPV genomic RNA, expressed as viral copies, was detected at high levels only in inflamed organs and

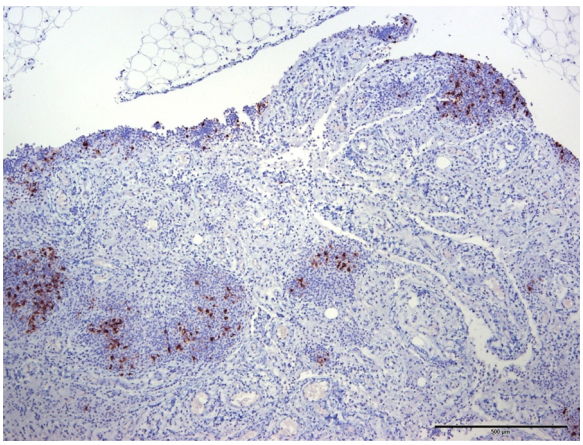

Fig. 8. Omentum stained for FIPV antigen (Immunoperoxidase). FIP antigen is present in inflammatory nodules and on the peritoneal surface.

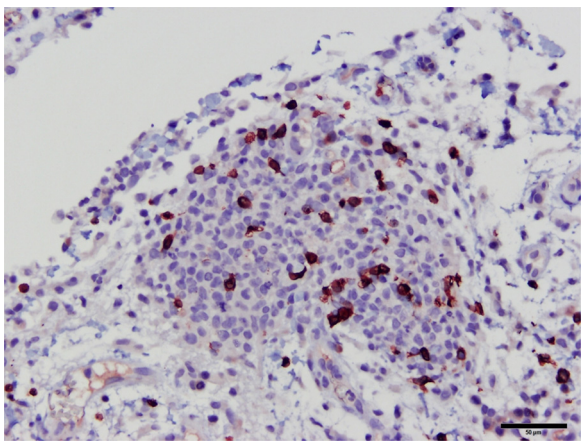

Fig. 10. Omentum (Immunoperoxidase). Immunoreactivity for CD3 demonstrates few T lymphocytes present in omental pyogranulomas (400×).

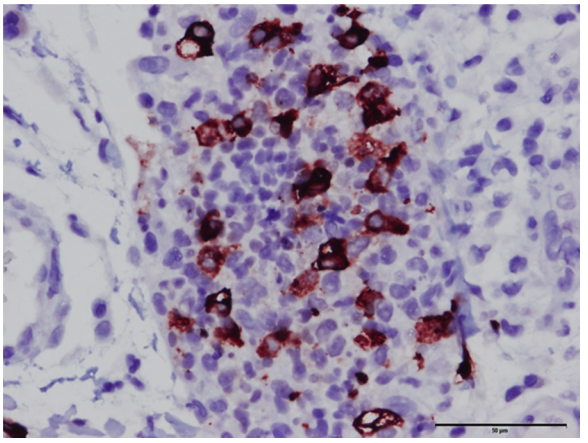

Fig. 11. Omentum (Immunoperoxidase): High magnification of an omental pyogranuloma shows a predominance of mononuclear cells. Immunopositivity for FIPV antigen is present in a population of large foamy macrophages (400×).

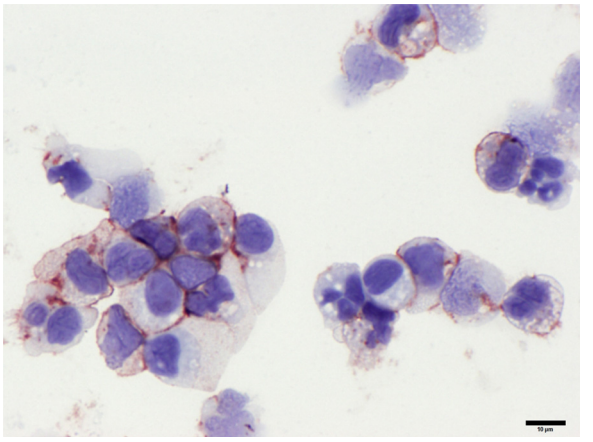

Fig. 13. Ascites fluid (Immunoperoxidase). Cytospin concentrated CD11b positive cells from FIP infected cat ascites fluid is comprised prodominantly of macrophages and lesser numbers of neutrophils. Macrophages demonstrate abundant membranous and variable cytoplasmic immunoreactivity for FIPV antigen by immunocytochemistry. Neutrophils are diffusely negative for FIPV.

effusion, while tissues from organs that did not appear to be grossly and histologically involved in the disease process frequently tested negative or were positive at much lower levels (Figs. 14 and 15). FIPV genomic RNA could not be detected from an identical set of tissues from two healthy cats (data not shown). The highest FIPV genomic RNA levels were in omentum, mesenteric lymph nodes, spleen and ascites, while low to negative levels were found in the kidney, lung, heart muscle, and popliteal lymph node. Viral genomic RNA was detected at variable levels in the liver and feces (Fig. 14). Although diarrheic stool had CT values ranging from 27.5 to 40.0 (3.94×10^6 to 3.57×10^2 FIPV genomes/g) and normal appearing stool 33–40 (8.87×10^4 to 3.57×10^2 FIPV genomes/g), the respective mean CT values were 34.8 and 34.3, indicating a lack of relationship between fecal virus shedding and diarrhea. FIPV genomic RNA was not detected in a 6-week fecal sample taken from the single surviving cat. A high level of viral genomic RNA was detected in the ascitic fluid and over 90–99% (10 to 100-fold greater) was cell-associated rather than in the supernatant (Fig. 15).

FIPV genomic RNA levels in whole blood, white cell fraction, and plasma collected prior to any feline coronavirus exposure had CT values ranging from 37 to 40.0 (Table 1). Therefore, only CT values $\leq$37 were considered to be reliably positive for blood.

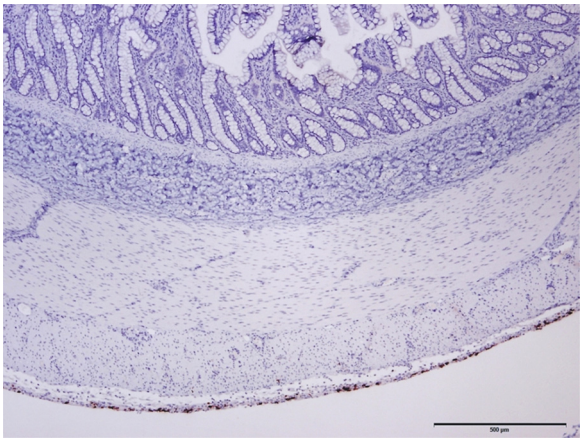

Fig. 12. Terminal ileum (Immunoperoxidase). FIP antigen is present within macrophages on the inflamed serosal surface, but is not observed in enterocytes.

4. Discussion

The clinical abnormalities, complete blood count changes, feline coronavirus antibody responses, and gross and histologic pathology were typical of experimentally induced and naturally occurring effusive abdominal FIP. The first sign of disease was fever appearing around 2 weeks post-infection followed by the more specific clinical signs of effusive abdominal FIP. The occurrence of fever coincided with the appearance of serum antibodies, as has been previously shown (Pedersen and Boyle, 1980; Weiss and Scott, 1981). There was no relationship between the magnitude of the antibody response and disease outcome, with the highest titer being found in one cat that lived 6 weeks before succumbing. The relationship between the onset of disease signs and appearance of

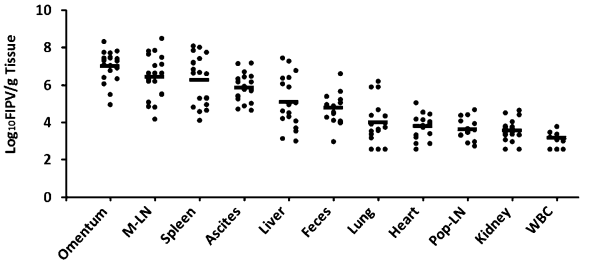

Fig. 14. Levels of FIPV genomic RNA in various tissues from cats experimentally infected with FIPV.

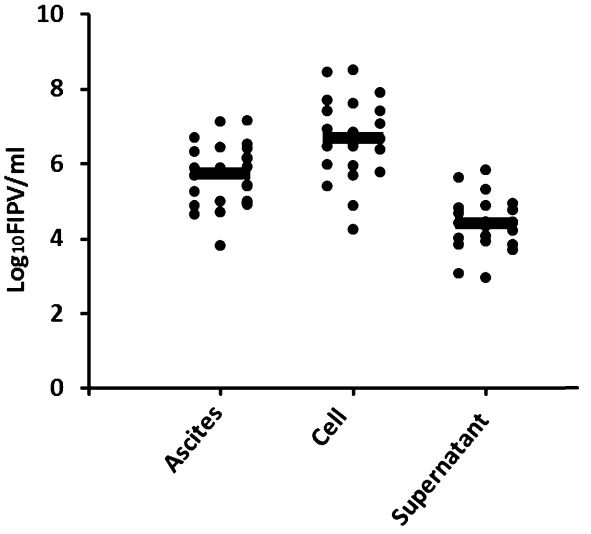

Fig. 15. Levels of FIPV genomic RNA in ascitic fluid from cats experimentally infected with FIPV.

antibodies was not coincidental. Previous studies have shown that virus neutralizing antibodies to S gene epitopes play a key role in enhancing disease by facilitating the uptake of FIPV by macrophages (Hohdatsu et al., 1998; Dewerchin et al., 2006) and participating in antigen/antibody/complement mediated vasculitis (Pedersen and Boyle, 1980; Jacobse-Geels et al., 1982). Antibody-dependent enhancement involving antibodies against S gene proteins has also been shown to play a role in SARS coronavirus infection (Wang et al., 2014).

The absolute lymphocyte count in blood was the most accurate predictor of disease outcome. The one surviving cat (P26) never manifested lymphopenia, while a second cat (P31) that survived for 6 weeks maintained near normal lymphocyte numbers until the last week of life. In contrast, the 18 cats that died within 4 weeks of infection demonstrated a precipitous drop in blood lymphocytes starting at 2 weeks post-infection. A similarly profound decrease in blood lymphocytes has been previously associated with disease signs in experimental FIPV infection (Dean et al., 2003), and varying degrees of lymphopenia are a common feature of naturally occurring FIP (Pedersen, 2009). Although T lymphocytes were entering diseased tissues, their proportion was low compared to macrophages and their numbers not appear sufficient to be solely responsible for the pronounced lymphopenia. Previous studies have associated lymphopenia in cats with experimentally induced FIP with a major apoptotic event (Dean et al., 2003). Apoptosis of lymphocytes has been implicated as a cause of lymphopenia and associated immunodeficiency in other virus infections (Razvi and Welsh, 1993).

Our finding that disease outcome in experimental FIP infection is associated with the degree of lymphopenia is in agreement with a conclusion made by de Groot-Mijnes et al. (2005), who studied experimental disease caused by the highly virulent type II FIPV-70-1146 – "Our combined observations suggest a model for FIP pathogenesis in which virus-induced T-cell depletion and the antiviral T-cell response are opposing forces and in which the efficacy of early T-cell responses critically determines the outcome of the infection." This conclusion has been mirrored by Fan et al. (2014), who postulated that "depending on intensity of the apoptosis of healthy cells, the apoptosis can either promote or comfort the long-term evolution of HIV infection."

We did not determine the lymphocyte subclasses that were most affected although the severity of the lymphocyte depletion suggested that both T and B subsets were involved. However, previous studies indicate that T cells, NK cells and T regs are most severely reduced in cats with naturally and experimentally induced FIP (Dean et al., 2003; Vermeulen et al., 2013).

Fecal levels of viral genomic RNA were low compared to what has been seen during primary infection with a field strain of FECV (Pedersen et al., 2008). Fecal virus in these FIPV infected cats ranged from around 1000 to 100,000 genomic RNA copies per gram of feces, far below levels detected in a single fecal swab during primary FECV infection (Pedersen et al., 2008). Although we did not determine the source of the fecal virus in these FIPV infected cats, it did not appear to be from enterocytes.

Immunohistochemistry failed to show infected enterocytes in either the ileum or caecum, sites of known virus replication during acute FECV infection (Pedersen et al., 1981; Meli et al., 2004). Moreover, enterocyte infection was not expected in these cats because the FIPV isolate used in this study had a truncated 3c gene and such mutants appear to have lost their ability to replicate in the intestinal epithelium (Chang et al., 2010; Pedersen et al., 2012). The viral RNA detected in feces was more likely to be a product of the intense inflammation that often involved the serosal surface of the intestines and often extended deeper into the intestinal wall in organs such as the ileum, caecum and colon. This conclusion was supported by the lack of fecal virus shedding in the one cat that never showed signs of disease.

The most significant findings in this study involved the relative paucity of viral genomic RNA detected in blood over the course of the infection and terminally in various tissues, which has direct implications on the use of RT-qPCR for diagnosing FIP from blood. It was not surprising to find high levels of virus terminally in grossly diseased tissues such as omentum, spleen and mesenteric lymph node and in abdominal effusions, and lower levels in organs such as liver, kidney, heart and lung that did not show gross parenchymal involvement. The levels of viral genomic RNA paralleled the intensity of the inflammatory response, which in turn paralleled the numbers of infected macrophages in the tissues or effusion. The selective targeting of macrophages by FIPV, which has been previously demonstrated (Pedersen and Boyle, 1980; Kipar et al., 1998), was reconfirmed by immunohistochemistry of heavily involved tissues such as the omentum, spleen, mesenteric lymph nodes and caecum, and ascitic fluid. Cells present in the ascitic fluid, which were predominantly macrophages, contained from 90 to 99% of the virus present in the each sample. The most parsimonious scenario would be that virus released from infected macrophages is immediately taken up by other macrophages and that this

cycle builds in intensity over time as more and more virus is produced and more and more macrophages either arrive from the blood as monocytes or proliferate locally from adventitial progenitors (Psaltis et al., 2014). The strict containment of an infectious agent in a single cell type such as macrophages is reminiscent of fastidious mycobacterial diseases of cats (Malik et al., 2013) and tuberculosis of humans (Mehrotra et al., 2014).

Although we failed to reliably detect coronavirus genomic RNA in blood at any stage of experimental infection with a field strain of Type I FIPV, others have reported a viremia using an identical RT-qPCR procedure (Gut et al., 1999). However, closer examination of these studies indicates that detection of feline coronavirus genomic RNA has not been as clear-cut as assumed, mainly because detection is often at or beyond the limits of reliability for the assay procedure. Three studies reported on the detection of feline coronavirus RNA in blood, but all were concerned with FECV rather than FIPV infection and detection was inconsistent (Meli et al., 2004; Kipar et al., 2010; Vogel et al., 2010). Kipar et al. (2001, 2006) compared virus loads in various tissues, excluding blood, in naturally infected cats and indicated that virus loads were higher in FIPV than FECV infected cats. Gunn-Moore et al. (1998b) used RT-PCR to detect FIPV genomic RNA in whole blood or plasma of 80–90% cats with FIP, both directly and after co-cultivation with WFE cells; plasma was just as likely to test positive as whole blood. However, they also found that 83–89% of healthy cats from FECV enzootic households also tested positive. de Groot-Mijnes et al. (2005) described a viremic phase in a subset of cats with FIP but virus loads were derived from RT-qPCR and RT-PCR data, as well as other data not shown. Moreover, virus levels where elevated usually at week one and terminally and were usually associated with CT values from 36 to 40. We conclude that viremia even in cats with highly fulminant experimentally induced FIP is either non-existent or below the reliable detection limits of highly sensitive RT-qPCR at all stages of the infection. Virus detection should concentrate on tissues and effusions containing FIPV infected macrophages.

Acknowledgements

Funding for this study was provided by the Center for Companion Animal Health, School of Veterinary Medicine, University of California, Davis, CA. Antibody and RT-qPCR testing was provided by IDEXX, Inc., West Sacramento, CA. We would like to thank Ms. Monica Durden and student helpers for providing excellent animal care.

References

Can-Sahna, K., Soydal Ataseven, V., Pinar, D., Oğuzoğlu, T.C., 2007. The detection of feline coronaviruses in blood samples from cats by genomic RNA RT-PCR. J. Feline Med. Surg. 9, 369–437.

Chang, H.W., de Groot, R.J., Egberink, H.F., Rottier, P.J., 2010. Feline infectious peritonitis: Insights into feline coronavirus pathobiogenesis and epidemiology based on genetic analysis of the viral 3c gene. J. Gen. Virol. 91, 415–420.

Chang, H.W., Egberink, H., Halpin, R., Spiro, D.J., Rottier, P.J., 2012. Spike protein fusion peptide and feline coronavirus virulence. Emerg. Infect. Dis. 18, 1089–1095.

de Groot-Mijnes, J.D.F., van Dun, J.M., van der Most, R.G., de Groot, R.J., 2005. Natural history of a recurrent feline coronavirus infection and the role of cellular immunity in survival and disease. J. Virol. 79, 1036–1044.

Dean, G.A., Olivry, T., Stanton, C., Pedersen, N.C., 2003. In vivo cytokine response to experimental feline infectious peritonitis virus infection. Vet. Micro. 97, 1–12.

Dewerchin, H.L., Cornelissen, E., Nauwynck, H.J., 2006. Feline infectious peritonitis virus-infected monocytes internalize viral membrane-bound proteins upon antibody addition. J. Gen. Virol. 87, 1685–1890.

Fan, R., Dong, Y., Huang, G., Takeuchi, Y., 2014. Apoptosis in virus infection dynamics models. J. Biol. Dyn. 13, 20–41.

Gunn-Moore, D.A., Caney, S.M., Gruffydd-Jones, T.J., Helps, C.R., Harbour, D.A., 1998a. Antibody and cytokine responses in kittens during the development of feline infectious peritonitis (FIP). Vet. Immun. Immunopath. 23, 221–242.

Gunn-Moore, D.A., Gruffydd-Jones, T.J., Harbour, D.A., 1998b. Detection of feline coronaviruses by culture and reverse transcriptase-polymerase chain reaction of blood samples from healthy cats and cats with clinical feline infectious peritonitis. Vet. Micro. 62, 193–205.

Gut, M., Leutenegger, C.M., Huder, J.B., Pedersen, N.C., Lutz, H., 1999. One-tube fluorogenic reverse transcription-polymerase chain reaction for the quantitation of feline coronaviruses. J. Virol. Methods 77, 37–46.

Herrewegh, A.A., de Groot, R.J., Cepica, A., Egberink, H.F., Horzinek, M.C., Rottier, P.J., 1995. Detection of feline coronavirus RNA in feces, tissues, and body fluids of naturally infected cats by reverse transcriptase PCR. J. Clin. Micro. 33, 684–689.

Hohdatsu, T., Yamada, M., Tominaga, R., Makino, K., Kida, K., Koyama, H., 1998. Antibody-dependent enhancement of feline infectious peritonitis virus infection in feline alveolar macrophages and human monocyte cell line U937 by serum of cats experimentally or naturally infected with feline coronavirus. J. Vet. Med. Sci. 60, 49–55.

Jacobse-Geels, H.E.L., Daha, M.R., Horzinek, M.C., 1982. Antibody immune complexes and complement activity fluctuations in kittens with experimentally induced feline infectious peritonitis. Am. J. Vet. Res. 43, 666–670.

Kipar, A., Bellmann, S., Kremendahl, J., Köhler, K., Reinacher, M., 1998. Cellular composition, coronavirus antigen expression and production of specific antibodies in lesions in feline infectious peritonitis. Vet. Immun. Immunopath. 65, 243–257.

Kipar, A., Köhler, K., Leukert, W., Reinacher, M., 2001. A comparison of lymphatic tissues from cats with spontaneous feline infectious peritonitis (FIP), cats with FIP virus infection but no FIP, and cats with no infection. J. Comp. Path. 125, 182–191.

Kipar, A., Baptiste, K., Barth, A., Reinacher, M., 2006. Natural FCoV infection: cats with FIP exhibit significantly higher viral loads than healthy infected cats. J. Feline Med. 8, 69–72.

Kipar, A., Meli, M.L., Baptiste, K.E., Bowker, L.J., Lutz, H., 2010. Sites of feline coronavirus persistence in healthy cats. J. Gen. Virol. 91, 1698–1707.

Malik, R., Smits, B., Reppas, G., Laprie, C., O'Brien, C., Fyfe, J., 2013. Ulcerated and nonulcerated nontuberculous cutaneous mycobacterial granulomas in cats and dogs. Vet. Dermatol. 24, 146–153.

Mehrotra, P., Jamwal, S.V., Saquib, N., Sinha, N., Siddiqui, Z., Manivel, V., Chatterjee, S., Rao, K.V., 2014. Pathogenicity of mycobacterium tuberculosis is expressed by regulating metabolic thresholds of the host macrophage. PLoS Pathog. 10, e1004265.

Meli, M., Kipar, A., Müller, C., Jenal, K., Gönczi, E., Borel, N., Gunn-Moore, D., Chalmers, S., Lin, F., Reinacher, M., Lutz, H., 2004. High viral loads despite absence of clinical and pathological findings in cats experimentally infected with feline coronavirus (FCoV) type I and in naturally FCoV-infected cats. J. Feline Med. Surg. 6, 69–81.

Pang, J., Modlin, J., Yolken, R., 1992. Use of modified nucleotides and uracil-DNA glycosylase (UNG) for the control of contamination in the PCR-based amplification of RNA. Mol. Cell. Probes 6, 251–256.

Pedersen, N.C., 2009. A review of feline infectious peritonitis virus infection: 1963–[2008]. J. Feline Med. Surg. 11, 225–258.

Pedersen, N.C., 2014a. An update on feline infectious peritonitis: virology and immunopathogenesis. Vet J., http://dx.doi.org/10.1016/j.tvjl.2014.04.017.

Pedersen, N.C., 2014b. An update on feline infectious peritonitis: diagnostics and therapeutics. Vet. J., http://dx.doi.org/10.1016/j.tvjl.2014.04.016.

Pedersen, N.C., Boyle, J., 1980. Immunologic phenomena in the effusive form of feline infectious peritonitis. Am. J. Vet. Res. 41, 868–876.

Pedersen, N.C., Boyle, J.F., Floyd, K., Fudge, A., Barker, J., 1981. An enteric coronavirus infection of cats and its relationship to feline infectious peritonitis. Am. J. Vet. Res. 42, 368–377.

Pedersen, N.C., Allen, C.E., Lyons, L.A., 2008. Pathogenesis of feline enteric coronavirus infection. J. Feline Med. Surg. 10, 529–541.

Pedersen, N.C., Liu, H., Dodd, K.A., Pesavento, P.A., 2009. Significance of coronavirus mutants in feces and diseased tissues of cats suffering from feline infectious peritonitis. Viruses 1, 166–184.

Pedersen, N.C., Liu, H., Scarlett, J., Leutenegger, C.M., Golovko, L., Kennedy, H., Kamal, F.M., 2012. Feline infectious peritonitis: Role of the feline coronavirus 3c gene in intestinal tropism and pathogenicity based upon isolates from resident and adopted shelter cats. Virus Res. 165, 17–28.

Pedersen, N.C., Liu, H., Gandolfi, B., Lyons, L.A., 2014. The influence of age and genetics on natural resistance to experimentally induced feline infectious peritonitis. Vet. Immunol. Immunopathol., http://dx.doi.org/10.1016/j.vetimm.2014.09.001.

Porter, E., Tasker, S., Day, M.J., Harley, R., Kipar, A., Siddell, S.G., Helps, C.R., 2014. Amino acid changes in the spike protein of feline coronavirus correlate with systemic spread of virus from the intestine and not with feline infectious peritonitis. Vet. Res. 45, 49.

Psaltis, P.J., Puranik, A.S., Spoon, D.B., Chue, C.D., Hoffman, S.J., Witt, T.A., Delacroix, S., Kleppe, L.S., Mueske, C.S., Pan, S., Gulati, R., Simari, R.D., 2014. Characterization of a resident population of adventitial macrophage progenitor cells in postnatal vasculature. Circ. Res. 115, 364–375.

Razvi, E.S., Welsh, R.M., 1993. Programmed cell death of T lymphocytes during acute viral infection: a mechanism for virus-induced immune deficiency. J. Virol. 67, 5754–5765.

Simons, F.A., Vennema, H., Rofina, J.E., Pol, J.M., Horzinek, M.C., Rottier, P.J., Egberink, H.F., 2005. A genomic RNA PCR for the diagnosis of feline infectious peritonitis. J. Virol. Meth. 124, 111–116.

Vermeulen, B.L., Devriendt, B., Olyslaegers, D.A., Dedeurwaerder, A., Desmarets, L.M., Favoreel, H.W., Dewerchin, H.L., Nauwynck, H.J., 2013. Suppression of NK cells and regulatory T lymphocytes in cats naturally infected with feline infectious peritonitis virus. Vet. Micro. 164, 46–59.

Vogel, L., Van der Lubben, M., Te Lintelo, E.G., Bekker, C.P.J., Geerts, T., Schuijff, L.S., Grinwis, G.C.M., Egberink, H.F., Rottier, P.J.M., 2010. Pathogenic characteristics of persistent feline enteric coronavirus infection in cats. Vet. Res. 41, 71.

Wang, S.F., Tseng, S.P., Yen, C.H., Yang, J.Y., Tsao, C.H., Shen, C.W., Chen, K.H., Liu, F.T., Liu, W.T., Chen, Y.M., Huang, J.C., 2014. Antibody-dependent SARS coronavirus infection is mediated by antibodies against spike proteins. Biochem. Biophys. Res. Commun., http://dx.doi.org/10.1016/j.bbrc.2014.07.090.

Ward, J.W., 1970. Morphogenesis of a virus in cats with experimental feline infectious peritonitis. Virology 41, 191–194.

Weiss, R.C., Scott, F.W., 1981. Antibody-mediated enhancement of disease in feline infectious peritonitis: comparisons with dengue hemorrhagic fever. Comp. Immunol. Microbiol. Infect. Dis. 4, 175–189.